

Nanoplastic in the North Atlantic Subtropical Gyre

Alexandra Ter Halle,^{*,†} Laurent Jeanneau,[‡] Marion Martignac,[†] Emilie Jardé,[‡] Boris Pedrono,[§] Laurent Brach,[†] and Julien Gigault^{*,†}

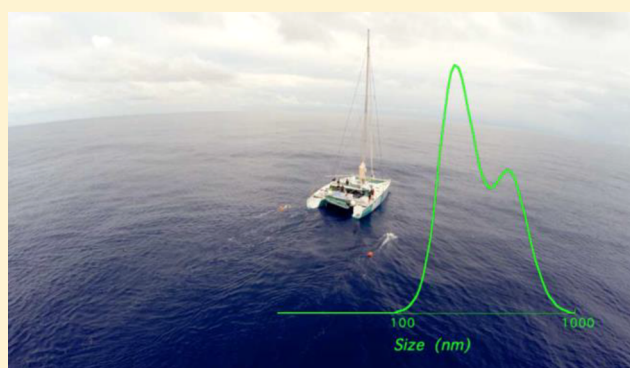
[†]Laboratoire des Interactions Moléculaires et Réactivité Chimique et Photochimique (IMRCP), UMR CNRS 5623, Université Paul Sabatier-UPS, Bâtiment 2R1, 3ème étage, 118, route de Narbonne, 31062 Toulouse Cedex 09, France

[‡]Laboratoire Géosciences Rennes, UMR6118 CNRS/Université de Rennes 1, 263 Avenue Général Leclerc, 35000 Rennes, France

[§]Cordouan Technologies, 11 avenue de Canterrane, 33600 Pessac, France

S Supporting Information

ABSTRACT: Plastics can be found in all ecosystems across the globe. This type of environmental pollution is important, even if its impact is not fully understood. The presence of small plastic particles at the micro- and nanoscales is of growing concern, but nanoplastic has not yet been observed in natural samples. In this study, we examined four size fractions (meso-, large micro-, small micro-, and nanoplastics) of debris collected in the North Atlantic subtropical gyre. To obtain the nanoplastic portion, we isolated the colloidal fraction of seawater. After ultrafiltration, the occurrence of nanoscale particles was demonstrated using dynamic light scattering experiments. The chemical fingerprint of the colloids was obtained by pyrolysis coupled with gas chromatography–mass spectrometry. We demonstrated that the signal was anthropogenic and attributed to a combination of plastics. The polymer composition varied among the size classes. At the micro- and nanoscales, polyvinyl chloride, polyethylene terephthalate, polystyrene and polyethylene were observed. We also observed changes in the pyrolytic signals of polyethylene with decreasing debris size, which could be related to the structural modification of this plastic as a consequence of weathering.



INTRODUCTION

Plastic debris affects all habitats worldwide.^{1–7} Once plastic items are discarded in the environment, they often end up in waterways and are ultimately transported to the ocean.^{1,2} Because most plastics undergo very slow chemical or biological degradation in the environment, the debris can remain in the ocean environment for years, decades or even longer.^{8,9} While dense debris accumulates on the sea floor,³ floating debris is transported over very large distances across oceans.^{1,2} Due to ultraviolet radiation in sunlight, physical wave forces and hydrolysis, plastic debris is broken down into smaller pieces.⁹ Microplastics are defined as debris smaller than 5 mm;¹⁰ it is estimated that at least 5.25 trillion pieces of microplastic float at sea, mainly in subtropical gyres, where they accumulate due to sea currents.²

The environmental impact of plastic pollution in oceans is poorly understood despite an increasing awareness of the problem. Nonetheless, it is estimated that this impact is wide-ranging. Plastic debris can entrap marine fauna,^{11,12} and debris is ingested by a wide variety of animals, ranging in size from plankton to marine mammals.^{13–17} Additionally, debris can cause the dispersal of microbial and colonizing species to potentially non-native waters¹⁸ and transport organic contaminants to marine organisms at multiple trophic levels.^{19–22}

Global plastic production reached 288 million metric tons in 2012,²³ and an estimated 4.8–12.7 million metric tons of plastic entered the ocean from waste generated on land in 2010.²⁴ The global microplastic distribution across the oceans has been estimated using circulation models, and the total mass of microplastics is estimated to be between 93 and 236 thousand metric tons,²⁵ but this amount only represents approximately 1% of the global plastic waste input to oceans in 2010.²⁴ Clearly, microplastics are lost from the sea surface. The pathways and mechanisms involved in these losses have not been identified, and various hypotheses have been proposed, such as fragmentation into smaller pieces or sinking. Understanding the severity of the effects of plastic pollution requires better knowledge of the associated mechanisms. Recently, special attention has been given to smaller debris, that is, microscopic debris, but reliable detection and quantification methods have yet to be developed.²⁶ Mesoplastics are defined as plastic debris within the 5 mm–20 cm range, while microplastics are defined to be less than 5 mm in size,

Received: July 18, 2017

Revised: November 7, 2017

Accepted: November 8, 2017

according to the NOAA workshop consensus definition.²⁷ However, as far as the authors are aware, the lower limit for the definition of microplastics remained undefined for a long time. Recently, two categories have been proposed: large microplastics in the 1–5 mm range and small microplastics defined as micrometric particles, that is, below 1 mm.²⁸ These categories were confirmed by Galgani et al.²⁹ and suggested for adoption by the European Marine Strategy Framework Directive (MSFD) (precisely, large microplastics were defined by the range 1–5 mm and small microplastics by the range 20 μm to 1 mm). Nanosized plastic particles are referred as nanoplastics (1–999 nm size range).³⁰ Nanoplastics have not been characterized in natural samples, but studies have shown that they can be generated from microplastics under laboratory conditions.^{30–32} Here, we present the characterization of colloidal fractions of seawater collected in the western North Atlantic Ocean in the plastic accumulation area, from which four samples were collected (Figure 1). In the colloidal fraction,

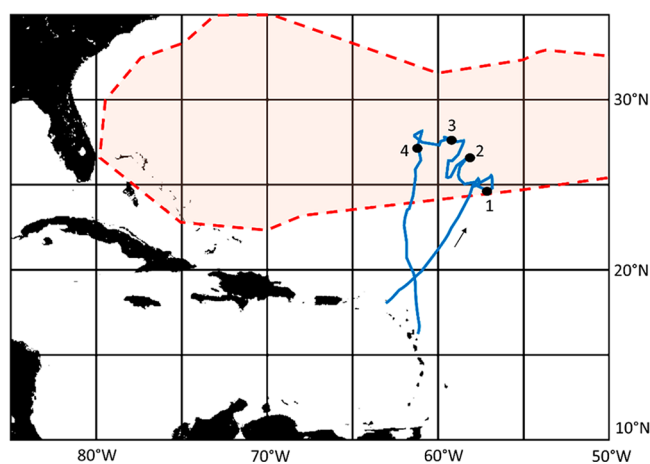


Figure 1. Cruise track of the 7th Continent Expedition in June 2015 in the North Atlantic Ocean (blue line). The plastic accumulation area was determined based on 30 years of in situ measurements by Law et al. (1) and is delimited using the dashed red line. The points indicate the sample locations (on the 2nd, 4th, 8th, and 11th of June 2015).

we consider particles that present colloidal behavior in aqueous systems, which includes nanoscale particles homogeneously dispersed in aqueous systems with sizes ranging from 1 nm to 1 μm . After ultrafiltration at a 10 000 Da molecular weight cutoff, we concentrated and characterized these colloids using in situ dynamic light scattering (DLS) and determined their chemical fingerprint by pyrolysis coupled with gas chromatography–mass spectrometry (Py-GC-MS).

EXPERIMENTAL SECTION

Chemicals. Six samples of polyethylene (PE) (CAS 9002–88–4) were obtained as reference materials. Three PE pellets were purchased from Sigma-Aldrich (Saint Louis, MO), including high density PE (HDPE) pellets presenting a melt flow index (MFI) of 2.2 g/10 min (this material is referenced as HDPE-2.2); HDPE pellets with an MFI of 12 g/10 min, a melting point between 125 and 140 °C and a density of 0.952 g mL^{-1} at 25 °C (referenced as HDPE-12); and linear low density PE (LLDPE) pellets presenting an MFI of 1.0 g/10 min, a melting point between 100 and 125 °C and a density of 0.918 g mL^{-1} at 25 °C (referenced as LLDPE-1). Three other PE samples were purchased from Goodfellow (Huntingdon,

UK): HDPE pellets (3 mm) with an MFI of 0.3 g/10 min (referenced as HDPE-3 mm); medium density PE (MDPE), which was a powder of 350 μm particles (referenced as MDPE-350 μm); and LDPE consisting of 1 mm pellets (referenced as LDPE-1 mm). Granular poly(ethylene terephthalate) (CAS 25038–59–9) with a density of 1.68 g mL^{-1} (referenced as PET) and poly(vinyl chloride) powder with a density of 1.4 g mL^{-1} at 25 °C (referenced as PVC) (CAS 9002–86–2) were purchased from Sigma-Aldrich. Granular (3.5 mm) polystyrene (CAS 9003–53–6, referenced as PS) and granular (3 mm) polypropylene (CAS 9003–07–0, referenced as PP) with an MFI of 0.4 g/10 min was purchased from Goodfellow (Huntingdon, UK). Several Polystyrene latex (PSL) standards from 100 to 1000 nm in size were purchased from Fisher Scientific (NIST-traceable Thermo Scientific Nanosphere Size Standard, Pittsburgh, PA).

Sample Collection. Seventeen mesoplastics (size range defined as 5 mm–20 cm, according to Andrady et al.⁸) were collected by the sailing vessel *Guyavoile* in the North Atlantic subtropical gyre in June 2015 during the French Expedition seventh Continent sea campaign. Large microplastics were collected using Neuston nets with a standard mesh size of 300 μm . The net consisted of a 0.5 \times 0.4 m rectangular frame fitted with a 2 m long net. Large microplastics were collected from the surface layer at a depth of 0–20 cm. Tow durations were set to 30 min, and tows were all undertaken while the vessel was traveling at a speed of 1–2.5 kn. On the boat, the contents of the tows were filtered on 300 μm sieves. Most of the plastic debris was removed with tweezers and stored at –5 °C in glass vials. In total 41 nets were towed, 10 outside the accumulation area and 31 within the accumulation area. Small microplastics were collected using a Neuston net with a standard mesh size of 25 μm . The net consisted of a 0.3 \times 0.1 m rectangular frame fitted with 3 m long net. Small microplastics were collected from the surface layer at a depth of 0–11 cm. Tow durations were set to 10 min and were all undertaken while the vessel was traveling at a speed of less than 1 kn. The content of the tows was filtered through a cellulose acetate membrane (5 μm) in a closed filtration unit, and then, the filters were stored in closed glass vials at –18 °C. Both manta nets were equipped with flow meters, from which sea surface concentrations could be calculated and expressed as the number of pieces per square kilometer. Colloidal fractions were obtained from seawater. Seawater was collected directly by plunging the glass bottles in the sea. The bottles were hand held to avoid any plastic equipment that could contaminate the samples. Brown 1 L glass bottles were prepared before the campaign. The bottles were washed three times with absolute alcohol and then three times with ultrapure water. The bottles were dried under a hood turned upside down on paper filter and finally sealed with a Teflon cap until use on site. The seawater samplings were taken on the tender at least 300 m from the boat after turning off the engine to avoid any contamination from gas exhaust. The bottles were rinsed three times with seawater before sampling one liter of seawater. The bottles were stored at room temperature. At each station, one liter of water was sampled.

Characterization of Mesoplastics. The mesoplastics were analyzed by infrared spectroscopy (see below for details of the settings).

Characterization of Large Microplastics. In addition to the first sorting of large microplastics on the boat under laboratory conditions using a binocular microscope (5 and 10 \times magnification), the smallest plastic debris was manually

separated from plankton. Afterward, plastic pieces were arranged in 20 cm diameter glass Petri dishes according to their size and color. Lines (fibers about one millimeter in diameter, attributed to fishing lines because clothing fibers are typically thinner³³) were treated separately and were measured manually with a ruler because they were often twisted. The Petri dishes containing the pieces were scanned. The image was treated with the ImageJ software. The pieces of plastic debris were individually identified, and their length and width determined. All plastic debris were then weighed to the nearest 0.01 mg. Finally, they were stored individually in glass vials at $-18\text{ }^{\circ}\text{C}$ for further characterization.

Characterization of Small Microplastics. In the laboratory, the membrane through which the content of the 25 μm mesh Neuston net was filtered was immersed in 80 mL ultrapure water at ambient temperature under gentle agitation for 1 h. After removal of the filter and to remove biogenic matter, 20 mL of a 10 M NaOH solution and 300 μL of a 50 g L^{-1} sodium dodecyl sulfate solution were added. Then, the solution was gently agitated for 4 h and stored for 1 week at ambient temperature. After 1 week, the solution was filtered through glass filters (Whatman GF/F; 0.7 μm ; 47 mm), which were stored in Petri dishes prior to analysis. A control experiment was performed to ensure that the plastic is not altered under these conditions. Briefly, 300 mg PE, PP, PVC, PS, and PET reference pellets were treated under the same conditions. After treatment, 95% ($\pm 5\%$) of the plastic was recovered. Under the microscope, the particles did not appear to be altered; for example, there was no yellowing. The micrometric particles on the filter were identified and counted using micro-Fourier transform infrared (micro-FTIR) spectroscopy using a Thermo Fisher Scientific Nicolet iN10 apparatus in reflection mode equipped with a liquid nitrogen-cooled MCT detector. The spectra were recorded as the average of 16 scans in the spectral range of 650–4000 cm^{-1} at a resolution of 8 cm^{-1} . The aperture was adapted to the micrometric particle size. All particles on the filter were individually detected under the FTIR microscope. Each particle was identified, measured under the microscope, and analyzed by FTIR microspectroscopy. For the particles suspected of being plastic, several measurements at different spots on the particles were undertaken to prevent the detection of false signals due to either local impurities or the rough and irregular shape of the debris, which could alter the infrared spectra. The plastic debris particles were identified using a polymer spectral library. The particles were determined to be microplastics if the polymer identification match was superior to 80%. The whole filter was analyzed to determine the heterogeneity of the samples, which is time-consuming and requires dozens of hours of analysis.

Colloidal Fraction Preparation and Characterization. The liter of seawater collected at each sampling site was first filtered through a 1.2 μm poly(ether sulfone) membrane (47 mm, Whatman) on a glass filtration unit. The filtered seawater (1 L) was then concentrated by ultrafiltration. Ultrafiltration at 10 kDa was conducted using an 8200-Amicon-stirred polysulfone-based cell (Milian, Ferney Voltaire, France with a 10 kDa membrane (poly(ether sulfone) membrane from Nadir, purchased with Alting, Metz, France). The samples were pushed through the membranes using N_2 at pressures varying from 40 to 100 kPa. Prior to use, all the membranes were washed and soaked in Milli-Q water. Before processing the sample set, the Amicon cell was thoroughly washed with Milli-Q water and dried upside-down under a hood on a paper filter

to avoid air contamination. The total volume of the filtration unit was 180 mL; consequently, during the ultrafiltration of 1 L of seawater, we had to stop the ultrafiltration, open the cell and refill it with seawater (the operation was repeated six times). For all the samples, we used the same procedure, and the final retentate volume was $10 \pm 2\text{ mL}$, which corresponds to the limit of the filtration procedure (i.e., just over the void volume of the system).

Microscope Imaging. Optical images were recorded using an Olympus BX53 microscope with a PLN X10 lens, and the images were processed with the Stream Basic software (Olympus Inc.).

Fourier Transform Infrared (FTIR) Spectroscopy. Infrared spectra were recorded using a Thermo Nicolet Nexus spectrometer equipped with a diamond crystal attenuated total reflectance (ATR) accessory and a deuterated triglycine sulfate (DTGS) detector. Background and sample spectra were acquired using 16 scans at a spectral resolution of 4 cm^{-1} . The recorded data were corrected to obtain transmission-like spectra using the ATR Thermo correction (assuming the refractive index of the sample to be 1.5). Infrared microscopy characterization was performed using a Thermo Scientific IN10. The nature of the plastic was determined using OmnicSectra (Thermo Scientific software, database: Hummel Polymer library, HR Polymer and additives, HR Polymer, additives and plasticizers).

Dynamic Light Scattering (DLS) Measurement. The in situ DLS measurements were performed using a Vasco Flex model nanoparticle size analyzer (Cordouan Technology, Pessac, France). The probe was placed in front of the ultrafiltration cell and measured directly in the solution. A long-term acquisition was optimized to obtain enough resolution from the baseline to characterize the entire colloidal size distribution. The limit of detection of the DLS instrument was investigated with PSL 100 nm standards within the range of $2 \times 10^{-5}\text{ g L}^{-1}$ to $2 \times 10^{-1}\text{ g L}^{-1}$ (see [Supporting Information \(SI\)](#)). Although detection is possible over the entire concentration range, an average size analysis is only possible over the concentration range of 2×10^{-2} to $2 \times 10^{-4}\text{ g L}^{-1}$ using the Padé-Laplace algorithm. For the most diluted sample ($2 \times 10^{-5}\text{ g L}^{-1}$), even if the presence of an autocorrelation function is identified, an average size analysis is not possible because the intensity of light is too close to that of ultrapure water (35 kcps). Each measurement corresponds to a statistical average of six measurements. In addition, each of the six measurements is composed of six acquisitions of light scattered for 80 s.

Pyrolysis, Thermodesorption and Thermochemolysis Coupled to Gas Chromatography–Mass Spectrometry.

A database of commercial polymers was made by analyzing six polymers from the list presented in the [Chemicals](#) section: LDPE-1 mm, HDPE-2.2, PVC, PET, PS, and PP. Plastic debris were analyzed over the size continuum from mesoplastics to colloidal fractions. For commercial plastics, mesoplastics and microplastics (approximately 10 μg) were introduced. For micrometric particles, 47 mm glass fiber filters were cut into eight pieces with prewashed scissors. The pieces were rolled and introduced in the 80 μL reactor one by one. For the colloidal fractions, the concentrated seawater after ultrafiltration was freeze-dried, and the remaining salts deposited on the glass vials were collected and crushed in an agate mortar for homogenization. Approximately 25 mg of lyophilizate was introduced to the 80 μL reactor and placed in a vertical

microfurnace pyrolyzer PZ-2020D (Frontier Laboratories). Pyrolysis was performed at 700 °C for 1 min, thermodesorption was performed at 300 °C for 1 min, and thermochemolysis was performed at 400 °C for 1 min in the presence of 10 mg of tetramethylammonium hydroxide (TMAH). Due to constraints on the available mass of lyophilizate, the thermodesorption and thermochemolysis experiments were performed only on the colloidal matter sampled on the 11th of June. Gases produced were injected directly into a GC-2010 (Shimadzu, Japan) equipped with an SLB 5MS capillarity column (60 m, 0.25 mm i.d., 25 μm film thickness) in split mode (nanoplastics: 5; micrometric particles: 10; meso-, micro-, and commercial plastics: 100). The temperature of the transfer line was 321 °C, and the temperature of the injection port was 310 °C. The oven temperature was initially 50 °C (held for 2 min), increased to 180 °C at 15 °C $\cdot\text{min}^{-1}$, and then increased to 310 °C (held for 44 min) at 5 °C $\cdot\text{min}^{-1}$. Helium was used as the carrier gas with a flow rate of 1.1 mL $\cdot\text{min}^{-1}$. After separation by GC, the compounds were detected by a mass spectrometer QP2010+MS (Shimadzu, Japan) operating in full-scan mode for m/z values between 50 and 600. The transfer line was at 280 °C, the molecules were ionized by electron impact using an energy of 70 eV, and the ionization source temperature was set at 200 °C. Identification of the molecules was achieved by comparison of their full-scan mass spectra with the National Institute of Science and Technology (NIST05 and NIST05s) library. Target compounds were determined to be present when the signal-to-noise ratio was higher than 3. Blank runs were performed between each analysis to avoid cross-contamination.

Treatment of the Chemical Fingerprint of Oceanic Colloids. Aromatic (22 compounds) and aliphatic (18 compounds) hydrocarbons were integrated using the m/z ratios listed in SI Table SII. The areas of the total ion chromatograms were approximated using the mass spectra factor (MSF) calculated as the reciprocal of the proportion of the m/z ratio used for integration and the entire fragmentogram of the NIST library.³⁴ The MSFs are listed in SI Table SII. These areas were used to determine the relative proportion of aliphatic and aromatic hydrocarbons in the analyzed compounds. This calculation corresponds to the proportions of individual compounds presented in SI Table S12.

Chemometric Approach to Determine the Proportions of PVC, PS, and PET. The proportion of PVC, PS, and PET in the aromatic fingerprint of nanoparticles was determined by a chemometric approach using principal component analysis (PCA). Such data-driven analysis is often used in environmental forensics studies.^{35,36} The statistical treatment was first developed using commercial plastics individual components. The variables were determined using a three-step procedure. First, the relative proportion of the 22 aromatic compounds detected in oceanic nanoparticles was determined in commercial plastics using total ion current (TIC) approximated areas. Then, only the molecules with a relative contribution of aromatic compounds higher than 0.5% in at least one plastic were chosen (13 molecules among 22). A first PCA was calculated with those 13 compounds. Redundant variables were removed by analyzing the correlation matrix calculated by the PCA treatment following a Pearson procedure with a 0.95 threshold. This third step conserved seven variables: benzene, toluene, C2 benzene, styrene, indene, naphthalene, and biphenyl. A 15% analytical uncertainty was included by adding two points per commercial plastic, which corresponds to

the analytical uncertainty in the reproducibility of the method for homogeneous samples. In this procedure, each plastic is defined by a surface and not a dot on the 2D diagram resulting from the PCA. On the plan composed of the two first factors, explaining 97.5% of the variance (F1:53.3% and F2:44.2%), PET, PVC, and PS are clearly separated. The relative proportions of the seven variables among the aromatic hydrocarbons determined in oceanic colloidal fractions were then included as additional individuals. Their coordinates were calculated without influencing the PCA. Their projections on the 2D diagram were included in the triangle defined by commercial plastics, with the exception of two replicates of the sample taken on the 11th of June. Assuming (i) that the chemical fingerprints of commercial PVC, PS, and PET are conserved and (ii) that those three plastics are the main contributors of the aromatic fingerprints of oceanic colloids, the proportions of chemical fingerprints of these three commercial plastics were calculated using an end-member mixing model. For the two samples plotted outside of the triangle, the proportion of PET was <0. This proportion was therefore fixed at 0, and the proportions of PVC and PS were calculated in such a way that their sum was 1.

Quality Assurance/Quality Control. Method blanks and controls were used to determine whether there was any contamination during sample processing. As sample processing was different with plastic debris size categories, controls and blanks were adapted for each protocol. The microplastics were sorted out with a stainless steel tweezer under a hood. For small microplastic, the main concern is airborne contamination and especially the deposition of synthetic fibers that could be released from clothing. On the boat, immediately after collecting the samples in the manta net, the content was transferred in a closed filtration unit. After filtration, the filter was placed with the use of a stainless steel tweezer in a closed glass vial and stored at -5 °C. The blank field consisted in filtering one liter of mineral water on the filtration unit. In the laboratory, in order to prevent contamination, we took the following measures: (i) the wearing of cotton lab coats, (ii) the use of gloves during sample processing, (iii) during filtration a glass cover was placed on top of the glass filtration unit to prevent airborne contamination, and (iv) all containers used for sample processing were cleaned using distilled water before use and turned upside down on a paper for drying. The process blank consisted in operating all the steps digestion/filtration/storage in parallel to sample processing and with the exact same procedure. Both field control and process control filters were inspected by micro-FTIR. The entire surface of the filters have been analyzed, just like the field samples. We did not detect any fibers on the control filters nor any plastic particles. For the colloidal fraction we took the same laboratory measures. But the main concern about the contamination of the nanoplastic comes from sample processing because we had no other choice than using membrane for filtration, membrane made of plastic. As a reminder, the protocol for the nanoplastics consisted in filtering 1L of seawater on 1.2 μm poly(ether sulfone) membrane (47 mm, Whatman) with the use a glass filtration unit. The seawater was, in a second step, concentrated by ultrafiltration using an Amicon stirred cell equipped with a 10 kDa poly(ether sulfone) membrane. To avoid any airborne contamination the glass unit filtration was closed with a glass plate and the Amicon cell is a closed unit. The procedural control consisted in collecting 1 L of ultrapure water in the same type of glass bottle equipped with a Teflon cap than for

sample collection. The ultrapure water was then filter on a 1.2 μm poly(ether sulfone) membrane and then concentrated by ultrafiltration on the Amicon cell. After concentration the presence of possible contamination was tested by DLS measurements. There was no presence of any colloids in the process control. Another control experiment was systematically performed, it consisted in the ultrafiltration of a solution of polystyrene latex standards under the same experimental conditions. This protocol allows determining if any size change can occur during the ultrafiltration process, indeed for some nanoscale materials ultrafiltration can induce change in the sample stability (aggregation characterized by a shift of the size distribution to the bigger size, that is, over 400 nm). We did not observe any aggregation of the polystyrene latex. Finally the quality control about the cross contamination by the membrane used for filtration and ultrafiltration consisted in Py-GC-MS investigation. The characteristic pyrolytic fingerprints of Teflon, and poly(ether sulfone), were not detected in the field samples (this is further discussed in the Discussion section). During Py-GC-MS analysis, blank runs were performed between each analysis to avoid cross-contamination.

RESULTS AND DISCUSSION

At sea, plastic pollution is generally evaluated based on large microplastic surface concentrations. Here, sampling was undertaken between 15 and 30°N and 55 and 65°W (Figure 1) and falls within the accumulation area determined by Law et al.¹ The large microplastic surface concentrations were between 10 000 and 250 000 pieces/km², which is typical in the North Atlantic subtropical gyre.¹ Seventeen mesoplastics were collected from the boat in the accumulation area: 10 were PE, 3 PET, 2 expanded PVC, 1 PS and finally 1 was wood. In total, from the 41 net tows dedicated to large microplastic sampling, 1099 pieces and 259 lines were collected. A randomly chosen 20% of the large microplastics were characterized by FTIR. In number, 90% of the large microplastics were made of polyethylene (PE), and 10% were made of polypropylene (PP). This is in agreement with previous studies in the North Atlantic subtropical gyre.³³ The small microplastics were quantified 8 times along the cruise in the accumulation area. In total, 1210 particles were identified, after matrix removal by micro-FTIR imaging, as synthetic polymers with acceptable certainty (a match of 80% with the spectral library). Interestingly the small microplastic sample contained a larger variety of polymers than the large microplastic sample. In number, the small microplastic sample was divided as follows: 73% PE, 13% PP, 8% PVC, 2% PS, and 1% PET. A priori, regarding the composition of the large microplastic sample (PE 90% and PP 10%), we did not expect such a diversity in polymer composition for the small microplastic sample. As a consequence, we performed a chemical procedure to remove biogenic matter using NaOH solution prior to micro-FTIR analysis. This chemical treatment led to a weaker alteration of the polymer than treatment with H₂O₂.³⁷ We controlled the treatment so that it did not alter PE, PP, PS, and PET. However, in view of the variety of the composition of the small microplastic sample, we recommend an enzymatic treatment for future studies.³⁸ Small microplastic concentrations ranged from 500 000 to 7 000 000 pieces/km². Note that these concentrations were significantly larger than the large microplastic concentrations. These concentrations are similar to the existing data (13–501 plastic debris per m³).³⁹

Dynamic Light Scattering (DLS) Measurement. To characterize the colloidal materials, the seawater was first

filtered at 1.2 μm and then analyzed by DLS, as illustrated in Figure 2. The autocorrelation curve of the filtered seawater

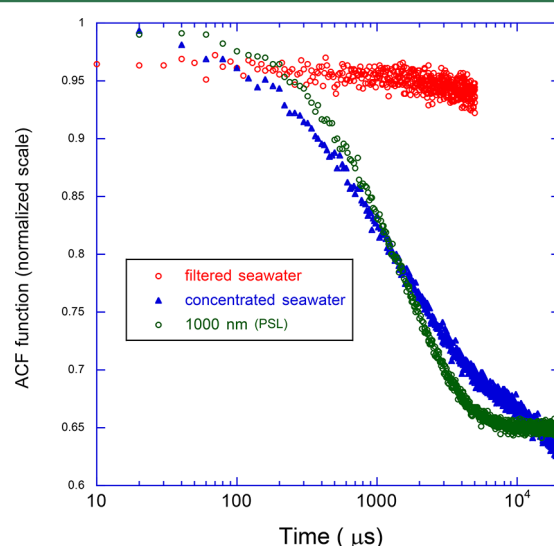


Figure 2. Autocorrelation function obtained by the in situ DLS analysis of the June 11th sample. The red points correspond to seawater after filtration at 1.2 μm . The blue points correspond to the retentate of seawater ultrafiltered with a molecular weight cutoff of 10 kDa (seawater concentrated 200 times). The green points correspond to polystyrene standards (PSL) of 1000 nm prepared under the same conditions based on the intensity of light scattered normalized by the size (in terms of photons collected).

yielded a constant signal of approximately 0.95, which indicates that no colloidal material could be detected in the samples. As expected, these results confirm that colloidal species in the open ocean are very dilute. Consequently, concentration by ultrafiltration at a molecular weight cutoff of 10 kDa was undertaken. The final retentate was concentrated 200 times. This step, in addition to concentration, allows the removal of dissolved organic matter under this cutoff level. The DLS analysis of the retentate yielded a relaxation of the light intensity over time, indicating the undeniable presence of colloidal materials in three of the samples. Due to sample dilution, it was still difficult to obtain an accurate size distribution, but the autocorrelation curve analysis indicated the presence of several populations of highly polydisperse particles on the nanoscale (1 to 1000 nm).

Pyrolysis Coupled to Gas Chromatography–mass Spectrometry. Py-GC-MS is widely used in the plastics industry to obtain structural information. This procedure has been applied in environmental studies for the evaluation of microplastics in natural samples^{37,40,41} and is applied in this study for the first time to investigate the occurrence of nanoplastics in the colloidal fraction of seawater. In addition, this analytical tool is also used in environmental studies to investigate the biogeochemistry of natural organic matter.^{42,43} The four sea samples analyzed presented reproducible and similar pyrolytic fingerprints (SI Table S11) and were composed of aromatic and aliphatic components (SI Figure S11). For the aromatic molecules, benzene was the most abundant compound, followed by toluene, styrene, and naphthalene (SI Table S11). The aliphatic fingerprint was composed of a series of linear hydrocarbons, from C₇ to C₁₉, with one or two unsaturations, and the intensity decreased as their length increased.

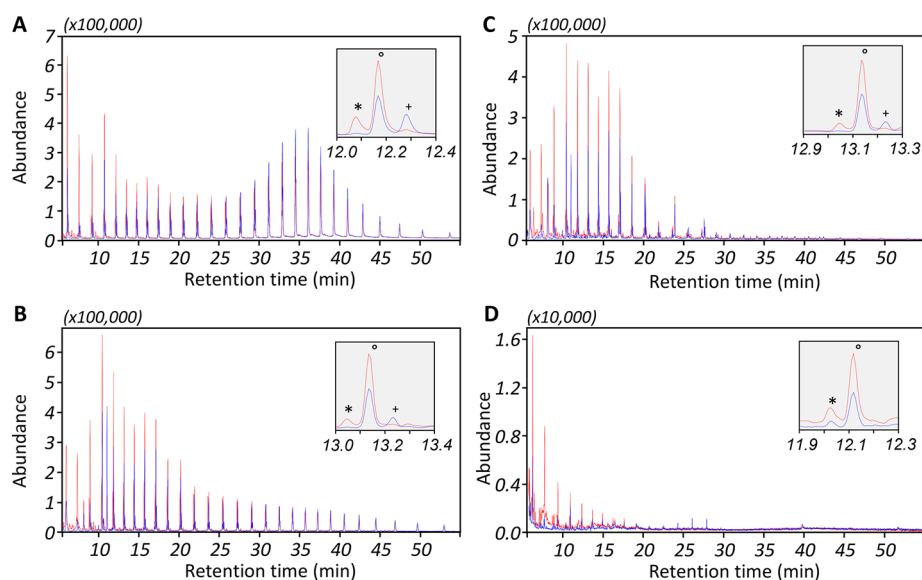


Figure 3. Single ion chromatograms ($m/z = 55$ in red and $m/z = 71$ in blue) of standard polyethylene (A) and plastic debris collected on June eighth; B: microplastics (0.3–5 mm); C: small microplastic (25–300 μm); and D: the seawater colloidal fraction. The magnified portion of each plot (shown in the box) highlights the triplet n -alkadiene *, n -alkene ° and n -alkane + triplet with 11 C atoms. The shift in retention times is due to differences in the column length due to weekly maintenance.

Aromatic and aliphatic hydrocarbons can be derived from the pyrolysis of natural marine colloidal organic matter. However, the pyrolysis of this environmental matrix yields mainly pyridines, amines and indoles from proteins and furans, as well as furaldehydes and cyclopentenones from carbohydrates.^{42,43} In the present samples, these compounds were not detected, probably because the initial volume of the samples (1 L) was not sufficient to detect natural marine colloidal organic matter. Due to the low concentration of marine colloidal organic matter, approximately 1 mg/L, the latest generation of high-resolution mass spectrometers requires at least 5 L of seawater to determine the composition.⁴⁴ Consequently, the pyrolytic fingerprint was considered to be anthropogenic.

The present pyrolytic fingerprint could result from plastics used during treatment, for example, from tetrafluoroethylene (TFE) from the sampling bottle caps and polysulfone (PSu) and poly(ether sulfone) (PESu) from the filtration and ultrafiltration membranes. The pyrolysis of TFE produces mainly fluorinated monomers, with depolymerization as the main pyrolytic mechanism.^{45,46} These compounds were not detected in the present samples; consequently, the anthropogenic fingerprint was not due to contamination by the sampling bottle caps. The filtration and ultrafiltration of deionized water did not produce any signal when analyzed by DLS. Moreover, the pyrolysis of PSu and PESu produces mainly phenol, diphenylether and 4,4'-sulfonylbis(phenoxybenzene),^{47,48} which were not detected in the present samples. Consequently, the pyrolytic fingerprint was not due to contamination during sample treatment but was characteristic of organic matter present in the samples. The fingerprint may result from the thermodesorption of persistent organic pollutants (POP) or from the pyrolysis of organic macromolecules, such as black carbon or plastics. The thermodesorption experiments at 300 °C did not yield the aromatic and aliphatic fingerprints obtained by pyrolysis. As a consequence, POP were not the source of the pyrolytic fingerprint of the colloidal organic matter. The pyrolysis and the thermochemol-

ysis with TMAH of aged black carbon yield high amounts of benzene, toluene and naphthalene.⁴⁹ To test this potential source of anthropogenic matter, the colloidal matter sampled on the 11th of June was analyzed by thermochemolysis with TMAH. Benzene, toluene and naphthalene were not detected in these experiments. However, trace amounts of benzoic acid methyl ester and two benzenedicarboxylic acid (B2CA) methyl esters (*ortho* and *para* isomers) were detected. Those compounds occurred in aged black carbon and are considered as markers of black carbon.⁴⁹ However, only the *meta*-B2CA isomer (not detected in this study) can be considered as a black carbon chemical marker since the *ortho* and *para* isomers have been detected in marine organisms.⁵⁰ Additionally, *ortho*-B2CA and *para*-B2CA are produced by the thermochemolysis of PET.⁵¹ Because (1) benzene, toluene and naphthalene were not detected by thermochemolysis and (2) the trace amount of *ortho*- and *para*-B2CA that was detected could be derived from the weak input of natural organic matter and/or from PET, the present anthropogenic fingerprint obtained by pyrolysis was attributed to plastics occurring in the colloidal fraction of the seawater samples.

A plastic database was prepared using the industrial polymers detected in the small microplastics fraction, that is, PE, PP, PVC, PS, and PET (SI Figure SI3). The chemical fingerprint of HDPE and LDPE were similar with a predominance (96% of the analyzed compounds) of a suite of triplet n -alkadiene, n -alkene, and n -alkane molecules ranging from n -C₇ to n -C₃₈ with a bimodal distribution. The first maximum was n -C₁₀ for both PEs, and the second was n -C₂₄ and n -C₃₀ for LDPE and HDPE, respectively. Benzene, toluene, C₂ benzene and styrene were also detected and represented 4% of the analyzed compounds. Such fingerprint is commonly described for the analytical pyrolysis of PE.⁴¹ The PP chemical fingerprint was dominated by branched and mainly unsaturated hydrocarbons, which represented 91% of the resolved peaks of the pyrograms. The main compound was 2,4-dimethylhept-1-ene, which is in accordance with previous studies.⁵² This compound was viewed in the colloidal fractions of seawater as a marker of PP. The

chemical fingerprint of PP also included aromatic hydrocarbons, namely, benzene, toluene and dimethylbenzene. The pyrolysis of PVC resulted in the production of aromatic hydrocarbons with the main products being benzene (72%), toluene (9%), naphthalene (7%), styrene and indene (2%). The pyrolysis of PET also yielded aromatic hydrocarbons, with the main products being benzene (80%), biphenyl (11%) and toluene (6%). The other detected hydrocarbons (dimethylbenzene, styrene and naphthalene) represented less than 1%. The chemical fingerprint of PS was dominated by styrene (71%), toluene and methylstyrene (9%) and benzene (4%). This predominance of styrene was reported for the Py-GC-MS of PS.⁴⁰ This database was used to determine the plastics in the colloidal fractions of seawater from the North Atlantic Subtropical gyre.

The aliphatic pyrolytic component of the colloids was composed of a series of linear hydrocarbons, from *n*-C₇ to *n*-C₁₉, which showed decreasing intensity as their length increased (Figure 3D). This pyrolytic fingerprint did not match the signal of any polymer from the database; however, the closest standard was PE. We compared the pyrolytic signals of mesoplastics (size between 20 cm and 5 mm), microplastics and small microplastics collected during the sampling campaign. The pyrolytic signals of the mesoplastics (Figure 3A) and large microplastics (Figure 3B) were similar to that of standard PE (SI Figure S13), but the second Gaussian distribution of hydrocarbons was attenuated in the large microplastic signal. Additionally, the second Gaussian distribution was largely attenuated in the small microplastic signal (Figure 3C). Depending on the small microplastic sample, the longest hydrocarbon detected varied from *n*-C₁₈ to *n*-C₃₈ (SI Figure S3). The shortening of the aliphatic chain length detected in the pyrolysis of micro- and nanoscale particles could be attributed to PE aging. Upon aging, PE exhibits structural modifications of the macromolecules (oxidation, shortening of the chains and other ramifications).^{32,33,53} These modifications are confined to the outer layer of the material (limited to 100 μm).^{32,33} Because microplastics are relatively large objects, the pyrolytic signature would not be affected by these surface alterations. The modification of the pyrolytic signal is perceptible for micrometric debris and is confirmed by the colloidal fraction. The aliphatic fingerprint was thus attributed to PE.

The molecule 2,4-dimethylhept-1-ene, a marker of PP, was not detected in the oceanic colloidal fractions. This indicates that PP is not present in the plastics occurring in these fractions, although it represented 10% of the plastics in the small microplastics fraction. This lack of PP detection could be due to (1) its effective low abundance in these fractions or (2) a modification of the pyrolysis products of nanoscale PP due to the smaller chains, similar to what was observed for PE.

The aromatic fingerprint was compared to the database of commercial polymers. The predominance of aromatic hydrocarbons was only found in the pyrolytic fingerprints of PVC, PET, and PS, which occurred in the small microplastic fractions. Based on the assumption that the aromatic signal of the colloids comes from a combination of the chemical fingerprints of these polymers, a chemometric approach using principal component analysis was applied. It was estimated that the colloidal aromatic fraction signal of seawater could be attributed on average to a mixture of 73% PVC (±18%), 18% PET (±16%), and 9% PS (±10%). The proportions for each sample are listed in Table 1. These proportions allow for the

Table 1. Proportions (%) of the Chemical Fingerprints of PVC, PS, and PET in the Aromatic Fingerprint of Oceanic Nanoparticles As Determined by PCA Followed by an End-Member Mixing Model

	06/02/2015	06/04/2015	06/08/2015	06/11/2015
PVC	63 ± 14	55 ± 8	80 ± 13	93 ± 7
PS	7 ± 4	20 ± 17	5 ± 3	5 ± 3
PET	31 ± 18	25 ± 14	14 ± 13	2 ± 4

calculation of a model aromatic fingerprint for the 12 analytical replicates. This fingerprint was compared to the measured aromatic fingerprint to examine the quality of the chemometric approach. The average of the residuals weighted by the relative proportion was 19.2%, suggesting a realistic approach. On the 2D plot obtained by PCA (Figure 4), two analytical replicates

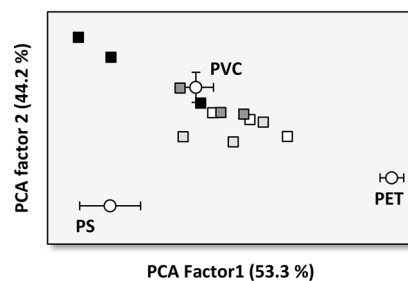


Figure 4. Projection on the 2D diagram defined by the two first factors of the PCA. These two factors explain 97.5% of the variance. End-members PVC, PET, and PS are represented by white circles, and oceanic colloidal fractions sampled on the 2nd, 4th, 8th, and 11th of June 2015 are represented by white, light gray, dark gray, and black squares, respectively. The three points per sampling dates correspond to analytical replicates.

of the colloidal fraction sampled on the 11th of June were plotted outside of the triangle formed by PVC, PS, and PET. This could be due to different factors: (1) even if present in trace amounts, natural organic matter may impact the statistical treatment; (2) the degradation of newly formulated synthetic polymers to colloidal plastics may modify the chemical fingerprint of the end-members; and (3) the area specific to each end-member may be larger due to heterogeneities in polymers formulated worldwide. In summary, the nanoplastic collected in the North Atlantic subtropical gyre were made of a combination of PE, PS, PVC, and PET. The small microplastics sampled in the same area were made of the same plastics, whereas the large microplastics were mainly made of PE (Table 2). This result indicates that although PE was supposedly estimated to be the most persistent polymer in marine environments, other polymers may degrade more rapidly and accumulate on the micro- and nanoscale. It is interesting to note the occurrence of PVC and PET at the micro- and nanoscale, which are denser than seawater. This finding suggests that the smallest plastic debris behaved differently than the microplastics, especially in terms of floatability.

As a conclusion, our preliminary data demonstrate the presence of nanoplastics in the North Atlantic subtropical gyre. These results raise up several questions on the degradation pathways of plastic litters and on the environmental fate of nanoplastics from their source to their final destination. There is currently an obvious limitation associated with sampling methods and characterization of the plastic particles at the micro- and nanoscale in natural samples to address the ongoing

Table 2. Average Proportion of Plastics among the Debris Collected during the Sea Campaign in the North Atlantic Subtropical Gyre According to Size Category (Percentage Given in Numbers)

	PE (%)	PP (%)	PS (%)	PVC (%)	PET (%)	wood (%)
mesoplastic (5 mm –20 cm)	59	17	12	6 ^a	nd	6
large microplastic (1 mm –5 mm)	90	10	nd	nd	nd	nd
small microplastic (20 μm–999 μm)	73	13	2	8	1	nd
nanoplastic (1–999 nm)	4	nd	9 ^b	70 ^b	17 ^b	nd

^aFoam PVC. ^bFor the nanoplastics, the proportion of plastic could not be calculated as the number of particles. The value is given as the mean of the relative proportion of the anthropogenic pyrolytic fingerprint. This number cannot be transformed into the proportion of plastics in the sample since the pyrolytic efficiency is not the same for each type of plastic.

questions. Are small microplastics and nanoplastics expected to accumulate in the same geographical area as microplastics? What about their subsurface distribution? We expect a different spatial distribution as they have different buoyant properties than large microplastics. It would also be particularly important to investigate the presence of anthropogenic nanoparticles in the natural water continuum from continents to oceans. What about the rate of fragmentation and oxidation of these small plastic particles? It would be important to know if there is accumulation of plastic at the micrometric and nanometric scale. On the contrary if nanoplastics are oxidized or fragmented faster than microplastics. These questions need to be considered urgently, and we hope that our work will help to promote/initiate them. Our team is currently involved in this research effort.

■ ASSOCIATED CONTENT

● Supporting Information

The Supporting Information is available free of charge on the ACS Publications website at DOI: 10.1021/acs.est.7b03667.

Figure SI1. Pyrolysis chromatograms of colloids sampled on the 11th of June 2015, Figure SI2. Single ion chromatograms of mesoplastics, microplastic, Figure SI3. Pyrograms of the commercial plastics, Table SI1 relative distribution of aliphatic and aromatic hydrocarbons by pyrolysis-gas chromatography–mass spectrometry analysis (PDF)

■ AUTHOR INFORMATION

Corresponding Authors

*(A.T.H.) E-mail: ter-halle@chimie.ups-tlse.fr.

*(J.G.) E-mail: julien.gigault@univ-rennes1.fr.

ORCID

Alexandra Ter Halle: 0000-0001-7065-2272

Emilie Jardé: 0000-0001-8108-4055

Julien Gigault: 0000-0002-2988-8942

Notes

The authors declare no competing financial interest.

■ ACKNOWLEDGMENTS

We thank the association Expedition seventh Continent for the sea sampling campaign, the staff and the crew. The authors are

also grateful to the association OSL. The project is supported by the Total Corporate Foundation, the Mission pour l'Interdisciplinarité of the Centre National de la Recherche Scientifique (CNRS), and the Centre National d'Études Spatiales (CNES, N°151168/02).

■ REFERENCES

- (1) Law, K. L.; Moret-Ferguson, S.; Maximenko, N. A.; Proskurowski, G.; Peacock, E. E.; Hafner, J.; Reddy, C. M. Plastic Accumulation in the North Atlantic Subtropical Gyre. *Science* **2010**, 329 (5996), 1185–1188.
- (2) Eriksen, M.; Lebreton, L. C. M.; Carson, H. S.; Thiel, M.; Moore, C. J.; Borerro, J. C.; Galgani, F.; Ryan, P. G.; Reisser, J. Plastic Pollution in the World's Oceans: More than 5 Trillion Plastic Pieces Weighing over 250,000 Tons Afloat at Sea. *PLoS One* **2014**, 9 (12).e11191310.1371/journal.pone.0111913
- (3) Schlining, K.; von Thun, S.; Kuhn, L.; Schlining, B.; Lundsten, L.; Stout, N. J.; Chaney, L.; Connor, J. Debris in the deep: Using a 22-year video annotation database to survey marine litter in Monterey Canyon, central California, USA. *Deep Sea Res., Part I* **2013**, 79, 96–105.
- (4) Ogata, Y.; Takada, H.; Mizukawa, K.; Hirai, H.; Iwasa, S.; Endo, S.; Mato, Y.; Saha, M.; Okuda, K.; Nakashima, A.; Murakami, M.; Zurcher, N.; Booyatumanondo, R.; Zakaria, M. P.; Dung, L. Q.; Gordon, M.; Miguez, C.; Suzuki, S.; Moore, C.; Karapanagioti, H. K.; Weerts, S.; McClurg, T.; Burres, E.; Smith, W.; Van Velkenburg, M.; Lang, J. S.; Lang, R. C.; Laursen, D.; Danner, B.; Stewardson, N.; Thompson, R. C. International Pellet Watch: Global monitoring of persistent organic pollutants (POPs) in coastal waters. 1. Initial phase data on PCBs, DDTs, and HCHs. *Mar. Pollut. Bull.* **2009**, 58 (10), 1437–1446.
- (5) Eriksen, M.; Mason, S.; Wilson, S.; Box, C.; Zellers, A.; Edwards, W.; Farley, H.; Amato, S. Microplastic pollution in the surface waters of the Laurentian Great Lakes. *Mar. Pollut. Bull.* **2013**, 77 (1–2), 177–182.
- (6) Zylstra, E. R. Accumulation of wind-dispersed trash in desert environments. *J. Arid. Environ.* **2013**, 89, 13–15.
- (7) Eerkes-Medrano, D.; Thompson, R. C.; Aldridge, D. C. Microplastics in freshwater systems: A review of the emerging threats, identification of knowledge gaps and prioritisation of research needs. *Water Res.* **2015**, 75, 63–82.
- (8) Andrady, A. L. Microplastics in the marine environment. *Mar. Pollut. Bull.* **2011**, 62 (8), 1596–1605.
- (9) Andrady, A., Persistence of plastic litter in the oceans. In *Marine Anthropogenic Litter*; Bergmann, M.; Gutow, L.; Klages, M., Eds.; Springer International Publishing, 2015; Part 1, pp 57–72.
- (10) Hidalgo-Ruz, V.; Gutow, L.; Thompson, R. C.; Thiel, M. Microplastics in the Marine Environment: A Review of the Methods Used for Identification and Quantification. *Environ. Sci. Technol.* **2012**, 46 (6), 3060–3075.
- (11) Laist, D. W. Overview of the Biological Effects of Lost and Discarded Plastic Debris in the Marine-Environment. *Mar. Pollut. Bull.* **1987**, 18 (6B), 319–326.
- (12) Wright, S. L.; Thompson, R. C.; Galloway, T. S. The physical impacts of microplastics on marine organisms: A review. *Environ. Pollut.* **2013**, 178, 483–492.
- (13) Cole, M.; Lindeque, P.; Fileman, E.; Halsband, C.; Goodhead, R.; Moger, J.; Galloway, T. S. Microplastic Ingestion by Zooplankton. *Environ. Sci. Technol.* **2013**, 47 (12), 6646–6655.
- (14) Cole, M.; Lindeque, P.; Fileman, E.; Halsband, C.; Galloway, T. S. The Impact of Polystyrene Microplastics on Feeding, Function and Fecundity in the Marine Copepod *Calanus helgolandicus*. *Environ. Sci. Technol.* **2015**, 49 (2), 1130–1137.
- (15) Sussarellu, R.; Suquet, M.; Thomas, Y.; Lambert, C.; Fabioux, C.; Pernet, M. E. J.; Le Goic, N.; Quillien, V.; Mingant, C.; Epelboin, Y.; Corporeau, C.; Guyomarch, J.; Robbens, J.; Paul-Pont, I.; Soudant, P.; Huvet, A. Oyster reproduction is affected by exposure to

- polystyrene microplastics. *Proc. Natl. Acad. Sci. U. S. A.* **2016**, *113* (9), 2430–2435.
- (16) Lusher, A. L.; Hernandez-Millan, G.; O'Brien, J.; Berrow, S. Microplastic and macroplastic ingestion by a deep diving, oceanic cetacean: The true's beaked whale *Mesoplodon mirus*. *Environ. Pollut.* **2015**, *199*, 185–191.
- (17) Lonnstedt, O. M.; Eklov, P. Environmentally relevant concentrations of microplastic particles influence larval fish ecology. *Science* **2016**, *352* (6290), 1213–1216.
- (18) Barnes, D. K. A. Biodiversity - Invasions by marine life on plastic debris. *Nature* **2002**, *416* (6883), 808–809.
- (19) Gouin, T.; Roche, N.; Lohmann, R.; Hodges, G. A Thermodynamic Approach for Assessing the Environmental Exposure of Chemicals Absorbed to Microplastic. *Environ. Sci. Technol.* **2011**, *45* (4), 1466–1472.
- (20) Beckingham, B.; Ghosh, U. Differential bioavailability of polychlorinated biphenyls associated with environmental particles: Microplastic in comparison to wood, coal and biochar. *Environ. Pollut.* **2017**, *220*, 150–158.
- (21) Koelmans, A. A.; Bakir, A.; Burton, G. A.; Janssen, C. R. Microplastic as a Vector for Chemicals in the Aquatic Environment: Critical Review and Model-Supported Reinterpretation of Empirical Studies. *Environ. Sci. Technol.* **2016**, *50* (7), 3315–3326.
- (22) Herzke, D.; Anker-Nilssen, T.; Nost, T. H.; Gotsch, A.; Christensen-Dalsgaard, S.; Langset, M.; Fangel, K.; Koelmans, A. A. Negligible Impact of Ingested Microplastics on Tissue Concentrations of Persistent Organic Pollutants in Northern Fulmars off Coastal Norway. *Environ. Sci. Technol.* **2016**, *50* (4), 1924–1933.
- (23) PlasticsEurope. *Analysis of European Plastics Production, Demand and Waste Data*; Association of Plastic Manufacturers: Brussels, 2014–2015; p 1–20.
- (24) Jambeck, J. R.; Geyer, R.; Wilcox, C.; Siegler, T. R.; Perryman, M.; Andrady, A.; Narayan, R.; Law, K. L. Plastic waste inputs from land into the ocean. *Science* **2015**, *347* (6223), 768–771.
- (25) van Sebille, E.; Wilcox, C.; Lebreton, L.; Maximenko, N.; Hardesty, B. D.; van Franeker, J. A.; Eriksen, M.; Siegel, D.; Galgani, F.; Law, K. L. A global inventory of small floating plastic debris. *Environ. Res. Lett.* **2015**, *10* (12), 124006.10.1088/1748-9326/10/12/124006
- (26) Filella, M. Questions of size and numbers in environmental research on microplastics: methodological and conceptual aspects. *Environ. Chem.* **2015**, *12*, 527–538.
- (27) Arthur, C.; Baker, J.; Bamford, H. *Proceedings of the International Research Workshop on the Occurrence, Effects, And Fate of Microplastic Marine Debris*, 2009.
- (28) Imhof, H. K.; Schmid, J.; Niessner, R.; Ivleva, N. P.; Laforsch, C. A novel, highly efficient method for the separation and quantification of plastic particles in sediments of aquatic environments. *Limnol. Oceanogr.: Methods* **2012**, *10*, 524–537.
- (29) Galgani, F.; Hanke, G.; Werner, S.; De Vrees, L. Marine litter within the European Marine Strategy Framework Directive. *ICES J. Mar. Sci.* **2013**, *70* (6), 1055–1064.
- (30) Lambert, S.; Wagner, M. Characterisation of nanoplastics during the degradation of polystyrene. *Chemosphere* **2016**, *145*, 265–268.
- (31) Gigault, J.; Pedrono, B.; Maxit, B.; Ter Halle, A. Marine plastic litter: the unanalyzed nano-fraction. *Environ. Sci.: Nano* **2016**, *3* (2), 346–350.
- (32) Lambert, S.; Wagner, M. Formation of microscopic particles during the degradation of different polymers. *Chemosphere* **2016**, *161*, 510–517.
- (33) ter Halle, A.; Ladirat, L.; Gendre, X.; Goudouneche, D.; Pusineri, C.; Routaboul, C.; Tenailleau, C.; Duployer, B.; Perez, E. Understanding the Fragmentation Pattern of Marine Plastic Debris. *Environ. Sci. Technol.* **2016**, *50* (11), 5668–5675.
- (34) Jeanneau, L.; Jaffrezic, A.; Pierson-Wickmann, A. C.; Gruau, G.; Lambert, T.; Petitjean, P. Constraints on the Sources and Production Mechanisms of Dissolved Organic Matter in Soils from Molecular Biomarkers. *Vadose Zone J.* **2014**, *13* (7), 010.2136/vzj2014.02.0015
- (35) Mudge, S. M. Multivariate statistical methods in environmental forensics. *Environ. Forensics* **2007**, *8* (1–2), 155–163.
- (36) Derrien, M.; Jarde, E.; Gruau, G.; Pourcher, A. M.; Gourmelon, M.; Jadas-Hecart, A.; Pierson-Wickmann, A. C. Origin of fecal contamination in waters from contrasted areas: Stanols as Microbial Source Tracking markers. *Water Res.* **2012**, *46* (13), 4009–4016.
- (37) Nuelle, M. T.; Dekiff, J. H.; Remy, D.; Fries, E. A new analytical approach for monitoring microplastics in marine sediments. *Environ. Pollut.* **2014**, *184*, 161–169.
- (38) Cole, M.; Webb, H.; Lindeque, P.; Fileman, E.; Halsband, C.; Galloway, T. Isolation of microplastics in biota-rich seawater samples and marine organisms. *Sci. Rep.* **2015**, *4*, 4528.
- (39) Enders, K.; Lenz, R.; Stedmon, C. A.; Nielsen, T. G. Abundance, size and polymer composition of marine microplastics $\geq 10 \mu\text{m}$ in the Atlantic Ocean and their modelled vertical distribution. *Mar. Pollut. Bull.* **2015**, *100* (1), 70–81.
- (40) Fabbri, D. Use of pyrolysis-gas chromatography/mass spectrometry to study environmental pollution caused by synthetic polymers: a case study: the Ravenna Lagoon. *J. Anal. Appl. Pyrolysis* **2001**, *58*, 361–370.
- (41) Fries, E.; Dekiff, J. H.; Willmeyer, J.; Nuelle, M. T.; Ebert, M.; Remy, D. Identification of polymer types and additives in marine microplastic particles using pyrolysis-GC/MS and scanning electron microscopy. *Environ. Sci.-Proc. Imp* **2013**, *15* (10), 1949–1956.
- (42) Sigele, A. C.; Hoering, T. C.; Helz, G. R. Composition of estuarine colloidal material: organic components. *Geochim. Cosmochim. Acta* **1982**, *46* (9), 1619–1626.
- (43) Sparkes, R. B.; Selver, A. D.; Gustafsson, O.; Semiletov, I. P.; Haghypour, N.; Wacker, L.; Eglinton, T. I.; Talbot, H. M.; van Dongen, B. E. Macromolecular composition of terrestrial and marine organic matter in sediments across the East Siberian Arctic Shelf. *Cryosphere* **2016**, *10* (5), 2485–2500.
- (44) Hansman, R. L.; Dittmar, T.; Herndl, G. J. Conservation of dissolved organic matter molecular composition during mixing of the deep water masses of the northeast Atlantic Ocean. *Mar. Chem.* **2015**, *177*, 288–297.
- (45) Hitz, J. A. Characterization of fluoroelastomers by various analytical techniques including pyrolysis gas chromatography/mass spectrometry. *J. Anal. Appl. Pyrolysis* **2014**, *109*, 283–295.
- (46) Ionfei, J.; Jingling, W.; Shuman, X. Mechanisms of pyrolysis of fluoropolymers. *J. Anal. Appl. Pyrolysis* **1986**, *10* (2), 99–106.
- (47) Crossland, B.; Knight, G. J.; Wright, W. W. A Comparative-Study of the Thermal-Stability and Mechanism of Degradation of Poly(Arylene Sulfones). *Br. Polym. J.* **1986**, *18* (3), 156–160.
- (48) Ohtani, H.; Ishida, Y.; Ushiba, M.; Tsuge, S. Thermally assisted hydrolysis and methylation-gas chromatography of poly(aryl ether sulfone)s in the presence of tetramethylammonium hydroxide. *J. Anal. Appl. Pyrolysis* **2001**, *61* (1–2), 35–44.
- (49) Kaal, J.; Brodowski, S.; Baldock, J. A.; Nierop, K. G. J.; Cortizas, A. M. Characterisation of aged black carbon using pyrolysis-GC/MS, thermally assisted hydrolysis and methylation (THM), direct and cross-polarisation C-13 nuclear magnetic resonance (DP/CP NMR) and the benzenepolycarboxylic acid (BPCA) method. *Org. Geochem.* **2008**, *39* (10), 1415–1426.
- (50) Dickens, A. F.; Gudeman, J. A.; Gelinias, Y.; Baldock, J. A.; Tinner, W.; Hu, F. S.; Hedges, J. I. Sources and distribution of CuO-derived benzene carboxylic acids in soils and sediments. *Org. Geochem.* **2007**, *38* (8), 1256–1276.
- (51) Dimitrov, N.; Krehula, L. K.; Sirocic, A. P.; Hrnjak-Murgic, Z. Analysis of recycled PET bottles products by pyrolysis-gas chromatography. *Polym. Degrad. Stab.* **2013**, *98* (5), 972–979.
- (52) Marin, N.; Collura, S.; Sharypov, V. I.; Beregovtsova, N. G.; Baryshnikov, S. V.; Kutnetzov, B. N.; Cebolla, V.; Weber, J. V. Copyrolysis of wood biomass and synthetic polymers mixtures. Part II: characterisation of the liquid phases. *J. Anal. Appl. Pyrolysis* **2002**, *65* (1), 41–55.
- (53) Ter Halle, A.; Ladirat, L.; Martignac, M.; Mingotaud, A. F.; Boyron, O.; Perez, E. To what extent are microplastics from the open ocean weathered? *Environ. Pollut.* **2017**, *227*, 167–174.